CHINESE OPTICS LETTERS
Vol. 21, No. 2 | February 2023

Continuously tunable CW single-frequency Nd:YAP/LBO laser with dual-wavelength output

Pixian Jin (靳丕铦)[1,2], Yi Cui (崔 艺)[1], Jing Su (苏 静)[1,2], Huadong Lu (卢华东)[1,2*], and Kunchi Peng (彭堃墀)[1,2]

[1] State Key Laboratory of Quantum Optics and Quantum Optics Devices, Institute of Opto-Electronics, Shanxi University, Taiyuan 030006, China

[2] Collaborative Innovation Center of Extreme Optics, Shanxi University, Taiyuan 030006, China

*Corresponding author: luhuadong@sxu.edu.cn

Received April 14, 2022 | Accepted August 15, 2022 | Posted Online September 16, 2022

We present a continuously tunable high-power continuous wave (CW) single-frequency (SF) Nd : YAlO$_3$/lithium triborate (Nd:YAP/LBO) laser with dual-wavelength output, which is implemented by combining an optimized and locked etalon with an intracavity nonlinear loss. The obtained output powers of the stable SF 1080 and 540 nm lasers are 2.39 and 4.18 W, respectively. After the etalon is locked to an oscillating mode of the laser, the wideband continuous frequency tuning and long-term stable single-longitudinal-mode operation of the laser are successfully realized, which can be well used for the applications of quantum information and quantum computation. To the best of our knowledge, this is the first realization of the continuously tunable high-power CW SF 1080/540 nm dual-wavelength laser.

Keywords: Nd:YAP laser; high power; continuous tuning; single frequency.

DOI: 10.3788/COL202321.021403

1. Introduction

Laser diode (LD) pumped all-solid-state continuous wave (CW) single-frequency (SF) lasers have been very essential light sources for precision measurement, quantum optics and information, atom-based applications, laser radar, and so on, which benefit from their intrinsic merits of low noise, high stability, and good beam quality[1]. Especially, a 1080 nm laser can realize type-II noncritical phase matching in a potassium titanyl phosphate (KTP) crystal[2], and, through a parametric down conversion process, the two-mode quadrature squeezed lights and a pair of Einstein–Podolsky–Rosen (EPR) entangled beams at 1080 nm can be directly generated just by pumping one nondegenerate optical parametric amplifier (NOPA) based on a type-II noncritical phase matched KTP crystal[3–5]. The scheme can be used for preparing the multi-partite continuous variable (CV) entangled states and establishing the complex quantum networks with a relatively simple implementation[6]. In the scheme, the second-harmonic wave (SHW) 540 nm laser serves as the pump light field, and the fundamental wave 1080 nm laser provides the local oscillation light for homodyne detectors and injected signal light field of the NOPA, so the CW SF 1080/540 nm dual-wavelength laser acts with a significant role in the scientific researches of quantum information and quantum computation. For preparing the multi-partite CV entangled states and establishing the quantum networks, more NOPAs and homodyne detectors are required, and then a CW SF 1080/540 nm dual-wavelength laser with high output power is desired. However, the severe thermal effect and fierce mode competition of the high-power 1080/540 nm laser as well as its frequency drift with the temperature fluctuation and airflow of the ambient environment under long-term operation can induce the occurrence of multi-longitudinal-mode (MLM) oscillation and mode-hopping of the laser, which inevitably influence the stability of the quantum optical experiment systems. To prevent the instability of the experiment system, an SF dual-wavelength laser with broadband mode-hop-free tuning ability is desired, so that the laser can easily keep stable single-longitudinal-mode (SLM) oscillation under long-term operation. In the quantum optics experimental system, the continuously tunable SF 1080/540 nm laser can also be used to adapt to different KTP crystals with slightly different phase-matching wavelengths and match with an ultra-low expansion (ULE) Fabry–Perot (F-P) cavity to reduce the intensity noise and frequency drift of the laser[7]. In addition, the tunable 1080 nm laser is also helpful for optical pumping of the atoms[8–11], where the continuous tunable SF 1080 nm laser is desirable for precisely matching its wavelength with the transition lines of the atoms, for example, the two-photon transition of cesium atoms (6S–7S)[10,11].

In 2013, Wang *et al.* reported a tunable CW SF microchip Nd : YAlO$_3$ (Nd:YAP) laser operating at 1080 nm, whose continuous tuning range covered 0.9 nm by varying the temperature of the gain medium[12]. However, the laser power was restricted within 155 mW, and, after the master oscillator power amplifier (MOPA) system, the laser power could be scaled to 1.4 W. For

© 2023 Chinese Optics Letters

the high-power 1080 and 540 nm lasers, the intracavity frequency-doubled Nd:YAP laser could be a feasible candidate. By this means, a high-power CW SF 1080/540 nm dual-wavelength laser with the output powers of 1.5 W at 1080 nm and 4.5 W at 540 nm was realized for preparing an eight-partite cluster state[13]. In contrast, to the best of our knowledge, a stable and continuously tunable high-power CW SF Nd:YAP laser has not been investigated to date. In this Letter, a continuously tunable high-power CW SF Nd:YAP/lithium triborate (LBO) laser with the output powers of 2.39 and 4.18 W at 1080 and 540 nm, respectively, was implemented by combining an optimized and locked etalon with the intracavity nonlinear loss introduced by the frequency-doubling process. After the etalon was successfully locked to an oscillating laser mode, and the laser cavity length was continuously scanned, the continuous laser frequency tuning with the potential tuning range of 314.03 GHz at 540 nm was realized, and a stable CW SF high-power 1080/540 nm dual-wavelength laser with long-term stable SLM operation was successfully obtained consequently.

2. Experimental Design

The designed continuously tunable high-power CW SF Nd:YAP/LBO laser with double-wavelength output is depicted in Fig. 1. The structure of the laser resonator was an '8' shape ring cavity formed by two plane-convex mirrors M_1 and M_2 with the curvature radii of 1500 mm and two plane-concave mirrors M_3 and M_4 with the curvature radii of 100 mm[13]. The input coupler M_1 was coated with anti-refection (AR) film at 803 nm and high-reflection (HR) film at 1080 nm. The mirror M_2 was HR coated at 1080 nm. The mirror M_3 was also HR coated at 1080 nm and mounted on a piezoelectric transducer (PZT). The output coupler M_4 was partially transmission coated at 1080 nm with the transmission of 1.5% and high-transmission coated at 540 nm. The pump source was a fiber coupled LD (FG-E001343, LIMO Lissotschenko Mikrooptik GmbH) with the maximal output power of 40 W, whose output wavelength was temperature tuned to 803 nm to match the stronger absorption peak of the laser gain medium. The pump laser beam output from the fiber with the numerical aperture of 0.22 and core diameter of 400 μm was focused into the laser gain medium by two lenses f_1 and f_2 with the focal lengths of 30 mm and 80 mm, respectively, which composed a telescope system. The laser gain medium was a Nd:YAP crystal cut along the *b* axis with the size of $\Phi 3\,\mathrm{mm} \times 15\,\mathrm{mm}$. The front end-face of the Nd:YAP crystal was coated with AR films both at 803 nm and 1080 nm. The other end-face of the crystal was coated with AR film at 1080 nm. An optical diode (OD) consisting of a terbium gallium garnet (TGG) crystal surrounded by a permanent magnet and a half-wave plate (HWP) was inserted into the laser resonator to ensure the unidirectional operation of the laser and eliminate the gain spatial hole burning. A type-I noncritical phase-matched LBO[14] with the size of 3 mm × 3 mm × 18 mm was positioned at the beam waist between M_3 and M_4 to achieve a high-frequency-doubling efficiency, and, simultaneously, the LBO crystal introduced a nonlinear loss[15,16]. The Nd:YAP, TGG, LBO crystals were wedge-shaped to eliminate their etalon effects and prevent their influence on the laser frequency tuning. An etalon mounted on the axis of a galvanometer scanner (GS) was inserted into the laser cavity as a mode selector and tuning element. By modifying the incidental angle of the etalon, the laser frequency could be coarsely tuned. To implement the continuous frequency tuning and enforce the long-term stable SLM operation of the laser, the transmission peak of the etalon had to be locked to the oscillating laser mode[17–19]. For this purpose, an etalon locking system located in the servo controller (SC) was adopted in the laser system, as shown in Fig. 1, and its operation principle was introduced in Ref. [20]. After the etalon was locked, the laser frequency could be continuously scanned just by applying a scanning signal or adjusting the bias signal in the PZT controlling system, where the signals were amplified (high-voltage amplifier, HVA) to match with the used PZT to automatically or manually scan the laser cavity length, respectively.

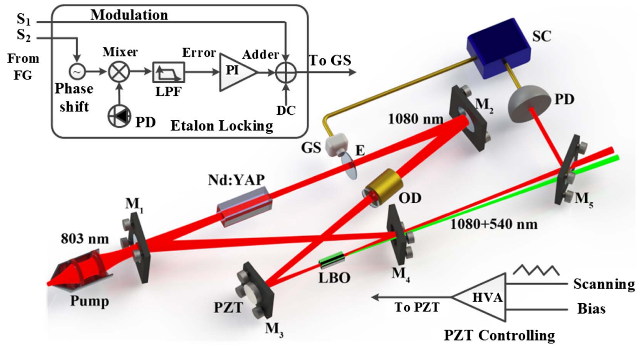

Fig. 1. Experimental setup of the continuously tunable high-power CW SF 1080/540 nm dual-wavelength laser. Nd:YAP, Nd:YAlO$_3$; GS, galvanometer scanner; E, etalon; SC, servo controller; OD, optical diode; PZT, piezoelectric transducer; LBO, lithium triborate; PD, photodetector; M$_{1-5}$, mirrors; FG, function generator; LPF, low pass filter; PI, proportion and integration; DC, direct current; HVA, high-voltage amplifier.

3. Experimental Results and Analysis

In the high-power lasers, the gain competition was fierce owing to the high gain and severe thermal effect of the laser crystal. In order to obtain SLM operation of the high-power Nd:YAP/LBO laser in the tuning process, the etalon used in the laser system should be carefully selected and designed, and the decisive parameter of the etalon was its bandwidth, which was defined as

$$\Delta\nu = \frac{\nu_{\mathrm{FSR}}}{F}, \tag{1}$$

where $\nu_{\mathrm{FSR}} = \frac{c}{2nd\cos\theta}$ was the free spectral range (FSR) of the etalon, which was decided by its thickness *d*, refractive index *n*, and light incident angle θ, and $F = \frac{\pi\sqrt{R}}{1-R}$ was the fineness of the etalon, which was decided by its reflectivity *R*. In experiment, an uncoated etalon made by quartz crystal with the thickness of 0.5 mm was first adopted, and the MLM oscillation of the laser was observed. When the etalon was coated with the reflection films with reflectivity of 12% at 1080 nm, the SLM operation of the laser was successfully achieved. The bandwidths of the above two etalons were 238.25 GHz ($d = 0.5\,\mathrm{mm}$, $R = 5.6\%$) and 152.44 GHz ($d = 0.5\,\mathrm{mm}$, $R = 12\%$), respectively, which revealed that the bandwidth of the utilized etalon should be at least narrower than 150 GHz to realize SLM operation of this tunable high-power Nd:YAP laser. Owing to the fact that the higher reflectivity of the etalon would lead to higher intracavity loss[21], to obtain a higher output power of the 1080/540 nm dual-wavelength laser, an uncoated quartz etalon with the thickness of 0.8 mm was designed and utilized in the laser system. The bandwidth of the etalon was 148.92 GHz ($d = 0.8\,\mathrm{mm}$, $R = 5.6\%$).

When the 0.8 mm thick etalon was adopted in the laser system, the output powers of the 1080 and 540 nm lasers versus the pump power were recorded. The output 1080 and 540 nm dual-wavelength lasers were separated by a dichroic mirror and injected into two power meters (PM30, Coherent Co., Ltd.). The recorded result is shown in Fig. 2. The threshold pump power of the laser was 29.5 W. The maximal output powers of 2.39 and 4.18 W at 1080 and 540 nm were obtained, respectively, at the incident pump power of 37.3 W, and the corresponding optical-to-optical conversion efficiency was 17.6%. When the incident pump power was 37.3 W, the laser power fluctuations at 1080 and 540 nm were recorded over 5 h with the sample rate of 1 sample per second, and the corresponding fluctuations were less than 0.11% (rms) and 0.27% (rms), respectively, as shown in Fig. 3(1). Simultaneously, the short-term laser power fluctuations were also measured by photodetectors (S3399 for 540 nm laser and ETX500 for 1080 nm laser) and observed in a digital oscilloscope (TDS2012B, Tektronix Co., Ltd.) with the measurement bandwidth up to 25 kHz. The obtained results showed that the short-term laser power fluctuations at 1080 and 540 nm were less than 0.136‰ (rms) and 0.233‰ (rms), respectively, which are shown in Fig. 3(2). The transverse-mode characteristic of the output 540 nm laser beam was also measured, and the measured values of M^2 in the x and y axes were 1.08 and 1.04, respectively, as shown in inset of Fig. 2.

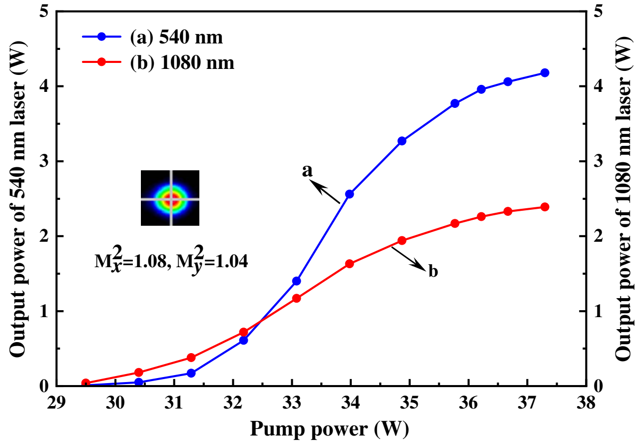

Fig. 2. Output powers of (a) 540 nm and (b) 1080 nm lasers versus pump power. Inset: spatial beam profile of output 540 nm laser.

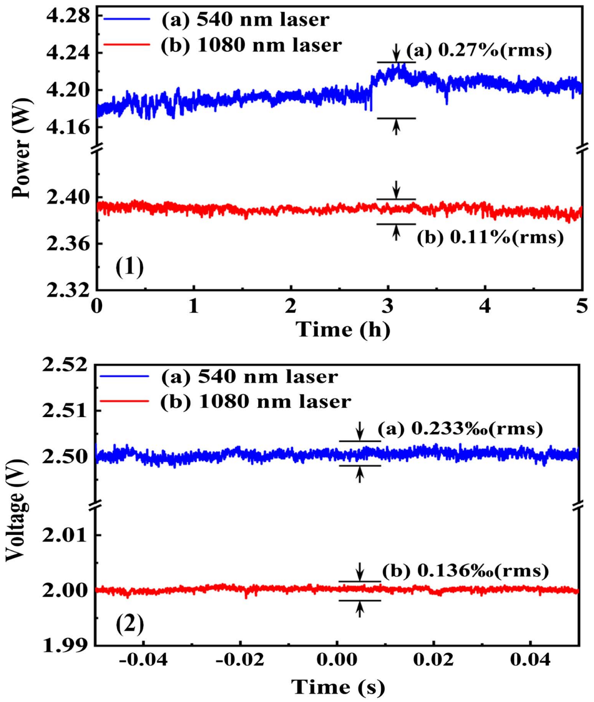

Fig. 3. Laser power stabilities at (a) 540 nm and (b) 1080 nm : (1) long-term, (2) short-term.

The tuning ability of the adopted etalon was then investigated by modifying its incidental angle to coarsely tune the laser wavelength, which was implemented by adjusting the voltage of the direct current (DC) signal applied to the GS in the SC. In this process, a fraction of the output SHW laser was injected into a wavelength meter (ws/765, High Finesse Laser and Electronic System) to monitor and record the output wavelength (or frequency) of the laser, and the recorded results are shown in Fig. 4. The results illustrated that the output wavelength of the laser could be tuned from 540.0834 to 539.8806 nm (and from 1080.1668 to 1079.7612 nm), and the FSR of the etalon was 210.8 GHz (for 540 nm laser) and 105.4 GHz (for 1080 nm laser). In this tuning process, the output power of the 540 nm laser fluctuated from 4.02 W to 4.27 W, as shown in Fig. 5. According to the maximum continuous frequency tuning range of the SF laser containing an intracavity locked etalon and a nonlinear loss element[22],

$$\nu_{\max} = \nu_{\mathrm{FSR}} + \frac{\left(\frac{\Delta\nu_H}{2}\right)^2}{2\nu_{\mathrm{FSR}}} \times \frac{\eta}{\eta + L}, \tag{2}$$

and the other parameters including the gain linewidth (ν_H) of 225 GHz for Nd:YAP crystal, the intracavity linear loss (L) of 7.5% and nonlinear loss (η) of 2.6%, the maximum continuous frequency tuning ranges of 167.22 GHz and 334.44 GHz for the 1080 and 540 nm lasers, respectively, were calculated.

In order to experimentally implement continuous frequency tuning of the designed laser, the transmission peak of the etalon

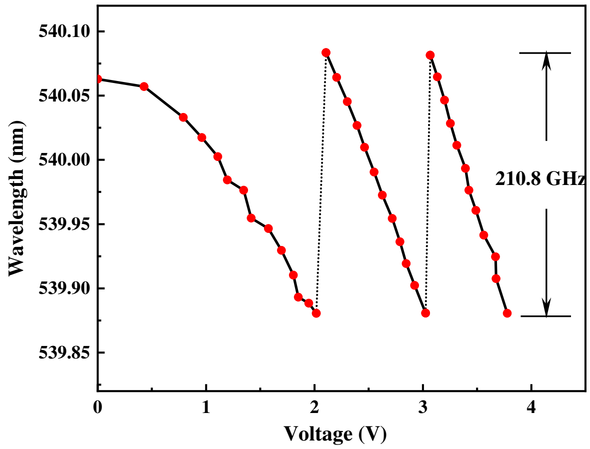

Fig. 4. Measured tuning range of utilized etalon.

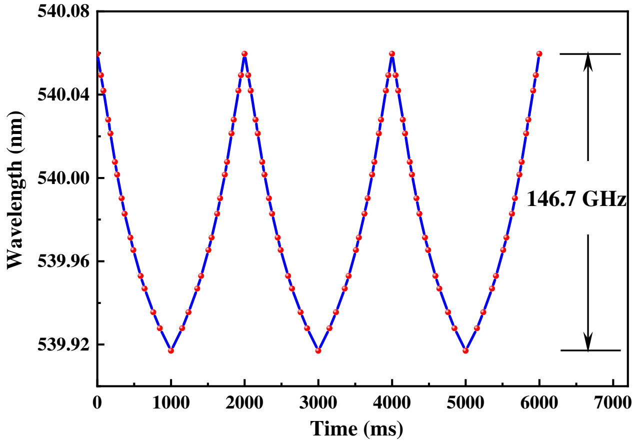

Fig. 6. Continuous frequency scanning of the laser.

was firstly locked to the oscillating mode with the wavelength of 540.0596 nm (and 1080.1192 nm) after the voltage of the DC signal was modified to 2.23 V. Subsequently, when a scanning signal with amplitude and frequency of 230 V and 0.5 Hz, respectively, was loaded onto the PZT to continuously scan the cavity length, the output wavelength of the laser could be continuously scanned from 540.0596 nm to 539.9170 nm with the corresponding frequency range of 146.7 GHz, as shown in Fig. 6, and the 540 nm laser power fluctuated with the same variation trend with its wavelength (or frequency), as shown in Fig. 5. The result showed that the obtained continuous frequency tuning range was less than the theoretically calculated value of 334.44 GHz, which was caused by the finite displacement of the PZT. In order to investigate the maximum continuous frequency tuning range of the designed laser, the etalon was locked to different oscillating wavelengths to realize continuous tuning of the laser, as shown in Fig. 7. The previous result was shown as curve (b) in Fig. 7. When the etalon was locked to the oscillating wavelength of 539.9201 nm after the DC voltage was adjusted to 2.84 V, the output wavelength of the laser could be continuously tuned from 539.9201 nm to 539.8148 nm, shown as curve (a) in Fig. 7, and then jumped to 540.0210 nm with the jump step of 212.2 GHz (at 540 nm), which corresponded to the FSR of the etalon. According to the analysis in Ref. [22], the wavelength of the laser reached the short-wave edge of its continuous tuning range at 539. 8148 nm, and, when the laser wavelength was continuously tuned to 539.8148 nm, its power decreased to 3.9 W. When the etalon was locked to the oscillating wavelength of 540.0589 nm after the DC voltage was adjusted to 2.235 V, the laser wavelength could be continuously tuned from 539.9201 nm to the long-wave side and reached the long-wave edge of its continuous tuning range at 540.1200 nm, shown as curve (c) in Fig. 7. When the laser wavelength was continuously tuned to 540.1200 nm, its power reached about 4.2 W. The experiment results revealed that the output wavelength of the laser could be continuously tuned from 540.1200 nm to 539.8148 nm if the variation of the cavity length was large enough, and the corresponding frequency range was 314.03 GHz, which agreed well with the theoretical analysis.

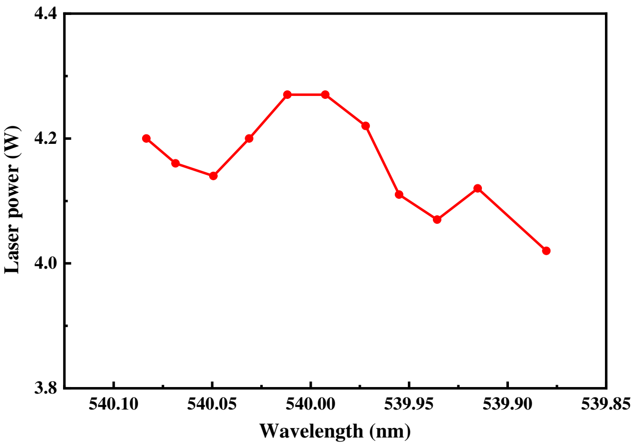

Fig. 5. Power fluctuation with laser wavelength.

Considering the optical cavity length of about 512 mm of the laser resonator, the continuous frequency scanning range of 314.03 GHz for the 540 nm laser corresponded to the variation

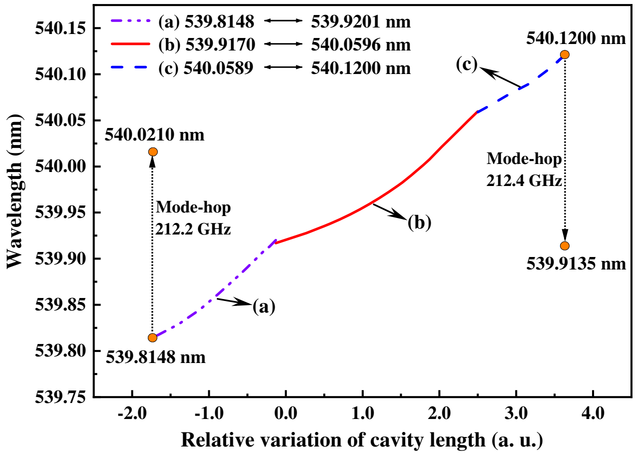

Fig. 7. Quasi-continuous frequency tuning of the laser over maximum tunable range.

of 290 µm of the cavity length, which indicated that the laser could maintain stable SLM operation when the variation of the laser cavity length was within the range of 290 µm in the long-term running process. In order to passively stabilize the laser system, the whole elements of the laser resonator were mounted in a duralumin monoblock construction. According to the thermal expansion coefficient of 23.6 ppm/°C for the duralumin materials, the cavity length variation of 290 µm corresponded to the ambient temperature fluctuation of 24°C, which manifested that the tolerability of the stable high-power SF 1080/540 nm laser for the ambient environment temperature fluctuation was ±12°C. For a common laboratory, the environment temperature fluctuation was generally less than ±12°C, so the obtained high-power 1080/540 nm laser could, in principle, maintain the stable SLM operation in long-term running, and, in addition, the laser could well adapt different operation environments with slightly different temperatures. In experiment, when the etalon was locked, the long-term stable SLM operation (over one day) of the laser was observed, and the total frequency drift was about 3 GHz. The experimental results revealed that the obtained high-power 1080/540 nm laser with stable SLM operation could be well used in the scientific researches of quantum information and quantum computation to guarantee the stability of the experiment system.

4. Conclusion

In summary, we presented a continuously tunable high-power CW SF Nd:YAP/LBO laser. When an uncoated quartz etalon with the thickness of 0.8 mm was chosen as the intracavity mode selector, the SF 1080 and 540 nm lasers with the output powers of 2.39 and 4.18 W were obtained, respectively, with the optical-to-optical conversion efficiency of 17.6%, which could be improved by adopting an etalon with lower reflectivity and appropriate thickness according to its bandwidth requirement and further optimizing the laser resonator. Combining the intracavity locked etalon and the nonlinear loss introduced by the frequency-doubling conversion, a continuously tunable 1080/540 nm laser with the potential tuning range of 314.03 GHz (at 540 nm) was realized and a 1080/540 nm laser with long-term stable SLM operation was successfully achieved. The tolerability of the obtained stable high-power CW SF 1080/540 nm laser for the ambient environment temperature fluctuation was ±12°C, so the obtained high-power CW SF laser could be well used in the applications of quantum information network and quantum computation.

Acknowledgement

This work was supported by the National Natural Science Foundation of China (Nos. 62105192, 61975100, and 62027821), Applied Basic Research Program of Shanxi Province (No. 201901D211186), Program for the Innovative Talents of High Education Institutions of Shanxi, and Fund for Shanxi "1331 Project" Key Subjects Construction.

References

1. Y. J. Wang, Y. H. Tian, X. C. Sun, L. Tian, and Y. H. Zheng, "Noise transfer of pump field noise with analysis frequency in a broadband parametric downconversion process," Chin. Opt. Lett. **19**, 052703 (2021).
2. V. M. Garmash, G. A. Ermakov, N. I. Pavlova, and A. V. Tarasov, "Efficient second harmonic generation in potassium titanate phosphate crystals with noncritical matching," Sov. Tech. Phys. Lett. **12**, 505 (1986).
3. P. D. Drummond and M. D. Reid, "Correlations in nondegenerate parametric oscillation. II. Below threshold results," Phys. Rev. A **41**, 3930 (1990).
4. Z. Y. Ou, S. F. Pereira, H. J. Kimble, and K. C. Peng, "Realization of the Einstein Podolsky Rosen paradox for continuous variables," Phys. Rev. Lett. **68**, 3663 (1992).
5. Y. Zhang, H. Wang, X. Y. Li, J. T. Jing, C. D. Xie, and K. C. Peng, "Experimental generation of bright two-mode quadrature squeezed light from a narrow-band nondegenerate optical parametric amplifier," Phys. Rev. A **62**, 023813 (1999).
6. X. L. Su, A. H. Tan, X. J. Jia, J. Zhang, C. D. Xie, and K. C. Peng, "Experimental preparation of quadripartite cluster and Greenberger–Horne–Zeilinger entangled states for continuous variables," Phys. Rev. Lett. **98**, 070502 (2007).
7. J. Yu, Y. Qin, Z. H. Yan, H. D. Lu, and X. J. Jia, "Improvement of the intensity noise and frequency stabilization of Nd:YAP laser with an ultra-low expansion Fabry-Perot cavity," Opt. Express **27**, 3247 (2019).
8. L. D. Schearer and P. Tin, "Tunable lasers at 1080 nm for helium optical pumping," J. Appl. Phys. **68**, 943 (1990).
9. W. G. Rellergert, S. B. Cahn, A. Garvan, J. C. Hanson, W. H. Lippincott, J. A. Nikkel, and D. N. McKinsey, "Detection and imaging of He_2 molecules in superfluid helium," Phys. Rev. Lett. **100**, 025301 (2008).
10. Y. L. Tian, P. F. Yang, W. Wu, S. K. Li, G. Li, P. F. Zhang, and T. C. Zhang, "Precision measurement of cesium 6S–7S two-photon spectra with single trapped atoms," Jpn. J. Appl. Phys. **58**, 042002 (2019).
11. H. Q. Yang, P. X. Jin, J. Su, X. D. Xu, J. Xu, and H. D. Lu, "Realization of a continuous-wave single-frequency tunable Nd:CYA laser," Chin. Opt. Lett. **20**, 031403 (2022).
12. X. Wang, T. Riesbeck, and H. J. Eichler, "Tunable single frequency microchip Nd:YAP MOPA laser operating at 1.08 µm," Laser Phys. **23**, 045804 (2013).
13. Y. J. Wang, Y. H. Zheng, C. D. Xie, and K. C. Peng, "High-power low-noise Nd:YAP/LBO laser with dual wavelength outputs," IEEE J. Quantum Electron. **47**, 1006 (2011).
14. Y. S. Zhang, J. Y. Zou, W. X. Zheng, K. Feng, B. Xu, and Z. F. Yu, "Watt-level continuous-wave intracavity frequency-doubled Pr:YLF-LBO laser at 320 nm," Chin. Opt. Lett. **19**, 091406 (2021).
15. K. I. Martin, W. A. Clarkson, and D. C. Hanna, "Self-suppression of axial mode hopping by intracavity second-harmonic generation," Opt. Lett. **22**, 375 (1997).
16. H. D. Lu and K. C. Peng, "Realization of the single-frequency and high power as well as frequency-tuning of the laser by manipulating the nonlinear loss," J. Quantum Opt. **21**, 171 (2015).
17. F. A. Camargo, T. Zanon-Willette, T. Badr, N. U. Wetter, and J.-J. Zondy, "Tunable single-frequency $Nd:YVO_4/BiB_3O_6$ ring laser at 671 nm," IEEE J. Quantum Electron. **46**, 804 (2010).
18. D. Radnatarov, S. Kobtsev, S. Khripunov, and V. Lunin, "240-GHz continuously frequency-tuneable/LBO laser with two intra-cavity locked etalons," Opt. Express **23**, 27322 (2015).
19. P. X. Jin, H. D. Lu, Y. X. Wei, J. Su, and K. C. Peng, "Single-frequency CW Ti: sapphire laser with intensity noise manipulation and continuous frequency-tuning," Opt. Lett. **42**, 143 (2017).
20. F. Q. Li, B. Zhao, J. Wei, P. X. Jin, H. D. Lu, and K. C. Peng, "Continuously tunable single-frequency 455 nm blue laser for high-state excitation transition of cesium," Opt. Lett. **44**, 3785 (2019).
21. W. R. Leeb, "Losses introduced by tilting intracavity etalons," Appl. Phys. **6**, 267 (1975).
22. P. X. Jin, H. D. Lu, Q. W. Yin, J. Su, and K. C. Peng, "Expanding continuous tuning range of a CW single-frequency laser by combining an intracavity etalon with a nonlinear loss," IEEE J. Sel. Top. Quantum Electron. **24**, 1600505 (2018).